




On Dual-Mode Driving Control Method for a Novel Unmanned Tractor with High Safety and Reliability

Wei Lu , *Member, IEEE*, Jiacheng Li , Huanhuan Qin, Lei Shu , *Senior Member, IEEE*,
and Aiguo Song, *Senior Member, IEEE*

Abstract—Due to the non-standardization and complexity of the farmland environment, it is always a huge challenge for tractors to achieve fully autonomy (work at Self-driving mode) all the time in agricultural industry. Whereas, when tractors work in the Tele-driving (or Remote driving) mode, the operators are prone to fatigue because they need to concentrate for long periods of time. In response to these, a dual-mode control strategy was proposed to integrate the advantages of both approaches, i.e., by combining Self-driving at most of the time with Tele-driving under special (complex and hazardous) conditions through switching control method. First, the state switcher was proposed, which is used for smooth switching the driving modes according to different working states of a tractor. Then, the state switching control law and the corresponding subsystem tracking controllers were designed. Finally, the effectiveness and superiority of the dual-mode control method were evaluated via actual experimental testing of a tractor whose results show that the proposed control method can switch smoothly, stably, and efficiently between the two driving modes automatically. The average control accuracy has been improved by 20% and 15% respectively, compared to the conventional Tele-driving control and Self-driving control with low-precision navigation. In conclusion, the proposed dual-mode control method can not only satisfy the operation in the complex and changeable farmland environment, but also free drivers from high-intensity and fatiguing work. This provides a perfect application solution and theoretical support for the intelligentization of unmanned farm agricultural machinery with high safety and reliability.

Index Terms—Dual-mode control, Unmanned tractor, Safety and Reliability, Tele-driving, Self-driving.

I. INTRODUCTION

THE population of the world is increasing and expected to reach 9.1 billion by 2050, however, the size of arable farmland on the earth is decreasing. To meet the globally increasing demand for food, the modern agriculture techniques such as precision farming and smart farming are utilized, whose essential part is the automation of agricultural

machinery to get higher efficiencies and better precisions for improving the productivity and quality of various field operation. Besides, the research on unmanned has become an important development direction of agricultural machinery, which is also in line with the demand for building intelligent and unmanned farms proposed in *14th Five-Year Plan for National Informatization* of China [1]–[3]. Various control techniques have been used for automation of agricultural machinery which can be divided into two modes called Self-driving and Tele-driving [4]–[7].

In this paper, the driving mode in which the machine works autonomously is called Self-driving (SD). It can improve the accuracy and efficiency of agricultural operations, reduce the costs of labor and fuel consumption [8]–[11]. However, it has potential safety hazards because the working path of farmland is complex and changeable dynamically, which is highly vulnerable to the external environment like rainstorm, fog, flood, drought, different crops and stages of growth. Besides, due to the existing technological limitation of artificial intelligence (AI), the tractors work in SD mode is more dangerous during field operation [12]–[15]. Therefore, it is difficult for unmanned tractors to complete high-quality farmland operations continuously in SD mode.

To ensure the operation of the unmanned tractor in the field as safe as possible, teleoperation technology has been introduced to agricultural vehicle driving remotely. Here, the driving mode that a tractor is controlled by a remote operator is named as Tele-driving (TD) [16]–[18], which can not only free the operator from high temperature, vibration and dust environment of the tractor cab, but also improve the reliability of farmland operations, reduce the working pressure of the farmer [19]–[21]. However, the TD mode requires real-time control by an operator, which still needs high intensity work.

Therefore, neither the SD mode nor the TD mode can satisfy the high efficiency and safety of the farmland operation simultaneously. Thus, to make up for the limitations of single-mode driving, a dual-mode control strategy was proposed to integrate the advantages of both approaches by combining SD with TD through switching control method [22]–[24] which can ensure the tractor works with high safety and reliability, and also reduce the work intensity of the operator as much as possible. Here, safety means that the tractor always works in the known and established states without losing control, and the reliability means that the tractor can still respond promptly to the switching control command and work well even under extreme conditions such as sensor signal loss, control command delay, and external signal interference. Fig.1

This work was supported in part by the Independent Innovation Project of Agricultural Science and Technology of Jiangsu Province (CX (20)3068), Modern Agricultural Machinery Equipment and Technology Demonstration and Promotion Project of Jiangsu Province (NJ2021-37), National Foreign Experts Program of China (G2021145010L), Science and Technology Project of Suzhou City (SNG2020039). (*Corresponding author: Wei Lu.*)

W. Lu, H. Qin and L. Shu are with the College of Artificial Intelligence, Nanjing Agricultural University, Nanjing 210031, China (e-mail: njaurobot@njau.edu.cn; qhuanhuan1001@163.com; lei.shu@njau.edu.cn).

J. Li was with Nanjing Agricultural University, Nanjing 210031, China. He is now with Unmanned System Research Institute, Northwestern Polytechnical University, Xian 710072, China (e-mail: jiacheng_li@mail.nwpu.edu.cn).

Aiguo Song is with the School of Instrument Science and Engineering, Southeast University, Nanjing, Jiangsu 210096, China (e-mail: a.g.song@seu.edu.cn).

Manuscript received October 06, 2021; revised April 24, 2022.

demonstrates the dual-mode driving system, which illustrates both the limitations of the current agricultural machinery operation and the advantages of the improved operation of the dual-mode driving system proposed in the paper.

A. Related Work

Till now, many studies and applications of the unmanned tractor have been carried out, which can be classified into two types 1) single-mode driving [25]–[33] and 2) dual-mode driving [34]–[44].

1) *Single-mode driving*: Many scholars have studied tractor tracking and navigation based on the planned path [25], [26]. To achieve mechanical operation with high reliability, several control methods of SD have been applied in the farmland. A. S. Matveev et al. used a nonlinear sliding mode control method in automatic path tracking of a tractor, which can solve the wheel slips problem effectively under the consideration of constraints on the steering angle [27]. A self-tuning fuzzy PID controller was utilized in the position tracking control of the tractor by W. Upaphai et al., which improved the performance of steering control response and path tracking accuracy [28]. Model predictive control (MPC) was used in the trajectory tracking control of an articulated unmanned ground vehicle by E. Kayacan et al., whose experimental results show the feasibility of their control method [29].

Teleoperation technology has also been applied in agricultural machinery for solving robot operation in complex and uncertain environment. A self-propelled sprayer used for tomato crops was introduced in [30], which is remotely controlled and monitored by radio signals to reduce the pesticides harm to workers and, meanwhile, to improve the efficiency of planting. The applications of remote control agricultural equipment in different farmland working environments were studied in [31] and [32], which show that the technology of remote control is suitable for reliable operation requirement of some special task in the farmland. To enhance the presence sense of the operator, a tractor driving simulator with immersive virtual reality was designed in [33], which can improve the efficiency of remote control and the safety of TD.

It is worth noting that in actual engineering operations, the system deviation is characterized as mutability and uncertainty due to human intervention under the TD mode [30]. However, high control accuracy can be achieved in the SD driving mode based on multi-sensor information fusion combined with autonomous control [9], [11]. Therefore, the control means, control objectives, and control requirements between the two models have significant differences.

2) *Dual-mode driving*: The application of dual-mode driving mainly exists in vehicle control, which is mostly based on the switch between controllers rather than the transformation of driving mode [34]–[37]. As for switching driving mode research, W. Wang et al. reviewed the researches on the shared control strategies between human drivers and automated driving agents and then pointed out that the human driver is an important part of the system [38]. C. Zhang et al. developed a remote-control system to assist the human's operation correspondingly by following a robot tractor using a human-driven tractor [39]. A continuously shared control method

was proposed in [40], which can provide driving assistance based on the control inputs of the driver and different driving situations to guarantee the safety of the vehicle. And the similar driving mode switching was also used in [41]–[44]. A semi-autonomous vehicle was proposed by B. Bashir et al. [42] to research the automation of man-machine systems under the consideration of the task differences between car and agricultural vehicles. For improving safety and reducing the agricultural operating costs, an automatic tractor was designed which does not stop until receiving commands from an operator over a wireless link when encountering obstacles or complicated road conditions [43], but it's inefficient and has little practical value. S. Ma proposed a modeling method that formulates the SD system as a switched system with unknown switch points to realize automatic driving of a vehicle, whose driving operation mode and their switch conditions are extracted simultaneously to make the vehicle complete conventional commands stably and efficiently [44], but it is still difficult to apply in the complex farmland environment.

B. Limitations and Challenges

It should be pointed out that a number of issues related to unmanned tractor driving are unclear, especially the research on reliability and safety, which are:

- 1) For the single mode control of unmanned tractor, the navigation-based SD has hidden danger, while the TD requires the operator to control all the time, which leads to high labor intensity and easy fatigue of the operator [22]–[24]. Therefore, the single-mode control method has great application limitations in large-scale farmland work.
- 2) As for dual-mode control of tractors, the existing researches mainly focus on a man-machine co-driving strategy, which means that tractors work in the unmanned driving mode at the most of time, and operators will intervene in control under complex working conditions. Local autonomous operation of tractors can be realized by the switching control [42], [43], [45], which can reduce working intensity of the drivers. However, the drivers are required to be on the tractor physically, which can not really improve the working environment of the operator.
- 3) There are many challenges from design to practical application of a dual-mode control unmanned tractor because an intelligent tractor is a complex intelligent unmanned system with interdisciplinary integration [13], [22], [26]. The entire research and development of this system involve sensing and detection theory, navigation and positioning theory, control theory, unmanned driving technology, practical engineering experience, farmland operations and its related knowledge [29].
- 4) Although many scholars have studied switching control theory of vehicle driving, due to the large differences between the assumptions in their paper and the actual complex engineering requirements [34]–[37], it is difficult to directly apply these methods to the actual engineering. Therefore, it's an important issue and real need

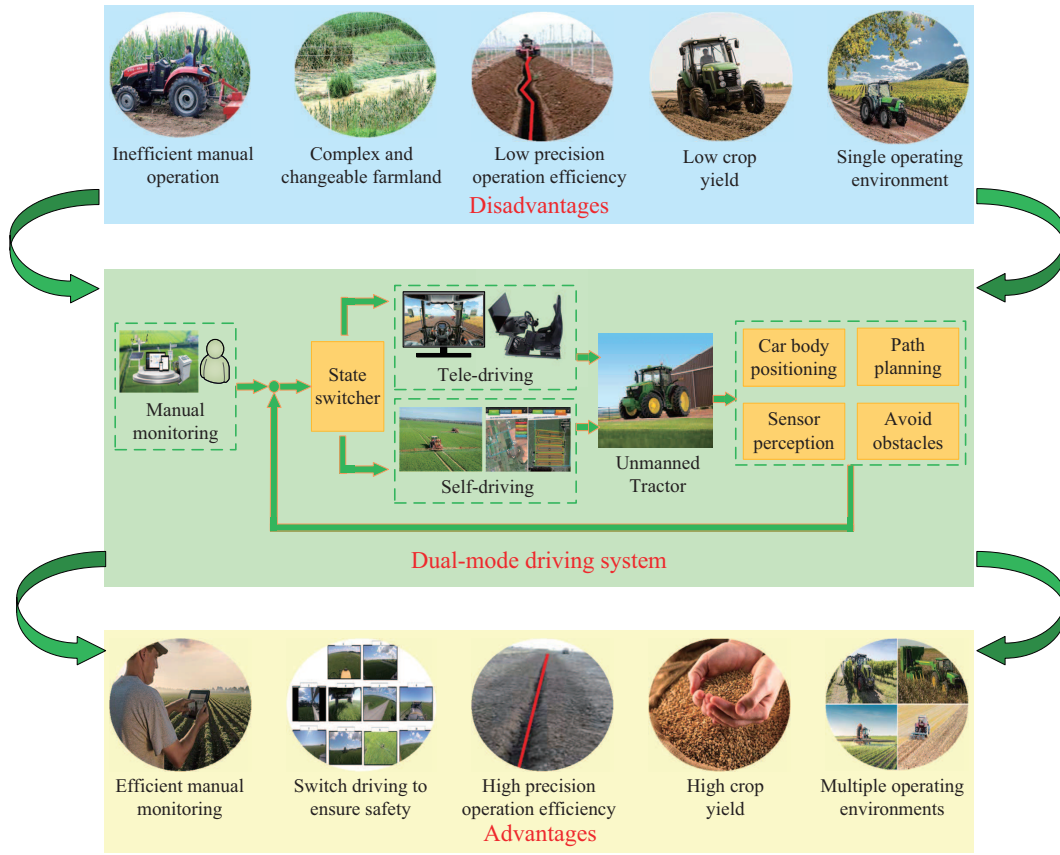


Fig. 1: Illustration of dual-mode driving system.

to design a suitable tractor switching control method for different driving modes in practical application, which may be based on the research of switching control.

C. Contributions and Characteristics

Based on the above discussion, design and realization of a dual-mode driving control method for the unmanned tractor with high safety and reliability were presented in this paper, which can fundamentally improve the limitations of the existing driving strategy. The contributions of this article are:

- 1) For practical agricultural engineering applications, the teleoperation technology of “human-in-loop” in the aerospace field [16], [18] was introduced to the field of agricultural robots in this paper. Combined with the tractor autonomous tracking operation technology, the dual-mode control system was constructed, which can be remotely monitored and controlled by the operator at any time. The dual-mode control tractor can not only meet the complex and changeable farmland environment, but also free the operator from the humdrum, high-intensity and complex work, which provides a perfect application solution for the intelligentization of farm agricultural machinery.
- 2) A set of driving switching logic with high safety and reliability was proposed in this article based on a large amount of theoretical knowledge and actual engineering experience in farmland, which can ensure the safety of

the tractor under any complex and uncertain farmland environment.

- 3) A novel unmanned tractor platform was built, which was upgraded from a traditional tractor by installing a driving robot on it to achieve rapid, nondestructive, intelligent upgrade of the traditional tractor. The unmanned tractor designed can work stably in both SD mode and TD mode, which provides a reliable and effective application platform for tractor intelligent driving control.

D. Organization

The rest of the paper is organized as follows: In Section II, some preparations were presented. The switching methods of the tractor were introduced in Section III. In Section IV, we designed the switching control algorithm and corresponding subsystem controllers for the two driving modes, respectively. In Section V, experiment results were presented to verify the effectiveness and superiority of the dual-mode control method of the unmanned tractor. Finally, Section VI concluded the paper.

II. BACKGROUND

A. Assumptions and Notations

Assumption 1: Assume that the effect of aerodynamics on the tractor can be ignored because of its slow speed.

Assumption 2: Assume that the tractor only moves in a plane parallel to the ground, which means that the movement

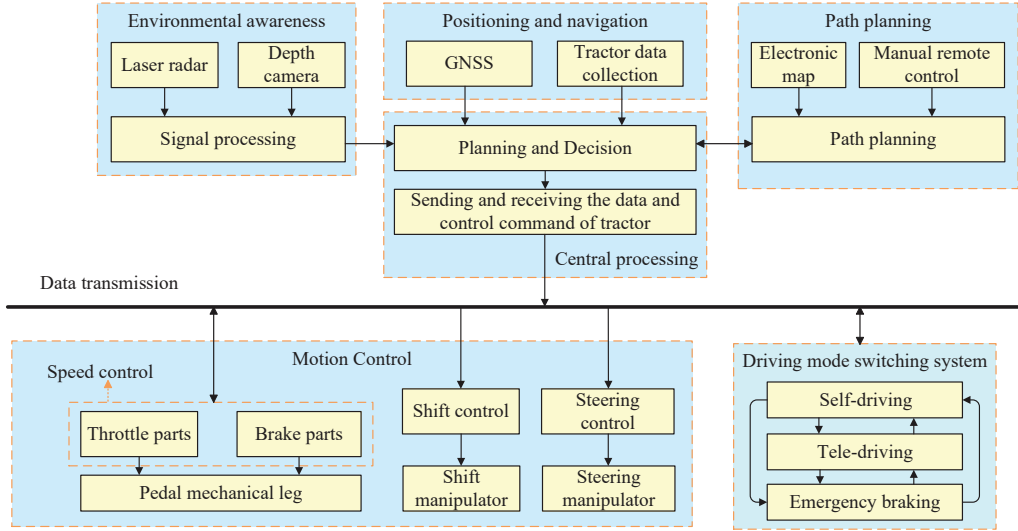


Fig. 2: The overall structure of SD subsystem.

of the tractor in the Z-axis direction, the roll motion around the X-axis and the pitch motion around the Y-axis are all ignored because the standardized farmland has been leveled.

Assumption 3: Assume the side slip angle of all the wheels of the tractor (α_f and α_r) and the wheel deflection angles (δ) are all small angles because the direction of the wheels steers slowly while working [45], [46].

Notations used in this paper were summarized in Appendix A.

B. Tractor Model

In this paper, the tractor was controlled based on the 2-DOF (Degrees of freedom) dynamic model, which can be expressed as

$$\dot{\mathbf{X}} = \mathbf{A}\mathbf{X} + \mathbf{B}\mathbf{u} \quad (1)$$

where the detailed modeling process was given in Appendix B.

Furthermore, the first-order difference quotient method was used to discretize the above model [47], [48], and the discrete state space expression was obtained as following

$$\mathbf{X}(k+1) = \mathbf{A}(k)\mathbf{X}(k) + \mathbf{B}(k)\mathbf{u}(k) \quad (2)$$

where, $\mathbf{A}(k) = \mathbf{I} + \bar{T}\mathbf{A}(t)$; $\mathbf{B}(k) = \bar{T}\mathbf{B}(t)$.

C. Self-driving

In the SD subsystem, a predefined route can be composed of the electronic maps. The GNSS (Global Navigation Satellite System) positioning and navigation unit is used to obtain tractor driving real-time information, which was fed back to the central processing unit for real-time path correction. The lidar unit is used to realize the obstacle avoidance driving function in the same time. To ensure the reliability of unmanned tractor farmland work, the technology of multi-sensor information fusion was used for improving the safety of the tractor. The overall structure of SD was shown in Fig. 2.

D. Tele-driving

The subsystem of TD consists of a master terminal (consisting of a monitoring, an operator, and a homogeneous virtual driver), a slave terminal (composed of a tractor driving robot), and cloud server. After the cloud platform was introduced, the master and slave can communicate with the cloud platform respectively, which can break through the distance limit and expand the local area network into a wide area network. In the same time, it can also enhance the signal transmission rate of teleoperation and improve the safety of driving robot. Moreover, virtual reality technology was applied to enhance the control immersion of the operator.

E. Communication

Specifically, all command transmissions are based on the TCP/IP protocol in the communication system to ensure the accuracy of command transmission. The UDP protocol is employed to ensure the real-time performance during video transmission and enhance the tele-presence of the operator. The communication principle of TD sub-system is based on the socket network communication principle, whose specific schematic diagram is shown in Appendix G.

III. DUAL-MODE SWITCHING METHOD

In this section, the state switcher and the corresponding switching control strategies were introduced.

A. Work Status of the Unmanned Tractor

During work time, the operator remotely monitors both the working state of the tractor and the visual information of its surroundings through video while the tractor works in unmanned driving mode. In addition, the sensors such as ultrasonic sensors and lidar set in the tractor are used for dynamic safety monitoring so as to initiate emergency brake action while encountering obstacles.

When the danger was detected by the operator or the obstacle avoidance alarm was detected by the sensor system,

the remote driving mode of “human-in-loop” will be switched to. In this way, unmanned driving in most of the time and remote driving in special conditions can be realized in the farmland. According to the actual farmland situation, we defined the following five working states of the unmanned tractor based on the TD and SD modes.

1) *State 1-Normal driving*: When a tractor works normally on a predefined route, the relationship between the wheelbase of tractor B , path curvature radius ρ and wheel deflection angle δ is

$$R = \frac{B}{\tan \delta} = \frac{1}{\rho} \quad (3)$$

where R is the turning radius and can be expressed as

$$R = \frac{1}{\rho} = \frac{(1 + y'^2)^{\frac{3}{2}}}{|y''|} \quad (4)$$

2) *State 2-Driving with small deviation*: When the tractor is affected by the damping moment of the farmland environment or other factors interfere to produce small deviation, the correction function is used to return the tractor to the set route. The correction function between lateral offset $\varepsilon(s)$ and wheel deflection angle $\delta(s)$ is

$$\frac{\delta(s)}{\varepsilon(s)} = \frac{h}{1 + \tau s} \quad (5)$$

where, h is the scale factor; τ is the delay time. Here, we set the limit delay time of the State 2 as λ_0 s ($\lambda_0 = 1$) [49], that means when the delay time exceeds λ_0 , the deviation satisfies the condition of large deviation.

3) *State 3-Driving with large deviation*: Large deviation refers to the big deviation between the longitudinal direction of the tractor and the navigation line direction. The position of the tractor should be adjusted while large deviation occurs. Here, the cubic spline interpolation is used to complete the road section where the tractor loses the signal. Based on the idea of piece-wise interpolation, 100 effective points of tractor coordinates closest to the breakpoint are used to create spline interpolation to construct smooth paths. The specific interpolation calculation process was introduced in the Appendix C.

4) *State 4-Tele-driving*: When the tractor has deviated from the scheduled route with a large deviation for a long time, it means that the ordinary correction method failed at that time, the machine is in the blind execution stage and needs to be switched to the TD mode. According to the existing experimental results of many scholars and actual needs of our tractor platform [50], we set the limit delay time of this subsystem as λ_1 s ($\lambda_1 = 3$). If the machine still cannot communicate and resume normal work after λ_1 s, the control mode will be switched immediately.

5) *State 5-Stop*: The stop state indicates the tractor is not working or stopped by emergency braking. Here, the emergency braking refers that the tractor stops immediately after receiving the braking command to ensure driving safety. Among them, the emergency braking command can come from the following three aspects:

- 1) Operator control: The operator can stop the unmanned driving system in any working state at any time.

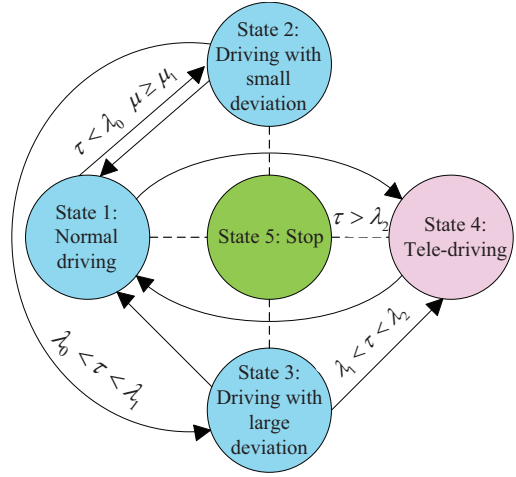


Fig. 3: Diagram of the state switcher.

- 2) Long-time loss of control signal: The tractor will stop moving when it cannot receive the tele-control signal and auto-control signal for a long time. Here, we set the limit time as λ_2 s ($\lambda_2 = 8$) [51], [52].
- 3) Encountered impassable obstacles: When the on-board sensor detects an obstacle, an alarm will be issued to stop the tractor in time.

B. State Switcher

According to previous research and data [53]–[55], the state switcher between the above five states was designed. In Fig. 3, μ is the input that represents the lateral deviation of the tractor from the predetermined path. When μ is not more than μ_1 ($\mu_1 = 0.1$ m), it can be determined that the tractor is moving on the predetermined path. When ρ is 0, the tractor works in the normal driving state which indicates the tractor is traveling in a straight line, and the steering angle θ is 0 at the same time; otherwise, the corresponding angle is calculated.

And when μ is greater than μ_1 , it can be determined that the tractor is currently deviating from the scheduled route, and the corresponding steering control is performed according to the measured delay time τ . When $\tau < \lambda_0$, the tractor is the travelling with small deviation, which can be adjusted by correction function. When $\lambda_0 < \tau < \lambda_1$, the tractor is moving with large deviation, the spline interpolation can be used to adjust the path. When $\lambda_1 < \tau < \lambda_2$, the TD mode should be switched to. When $\tau > \lambda_2$, the tractor must stop urgently.

C. Switch standards

Differently from the fixed-time [56] and finite-time [57] stability issues, the switching driving logic in this paper is mainly based on the lateral deviation and the delay time, which has many advantages of the stability problem. Considering the possible signal interruption of GNSS influenced by external environmental such as tree shade, the suitable switching standards are defined to ensure the safety of the unmanned tractor.

GNSS sampling interval is set to ξ s ($\xi = 0.01$). When the number of the signal interruption point exceeds n_{max} ($n_{max} =$

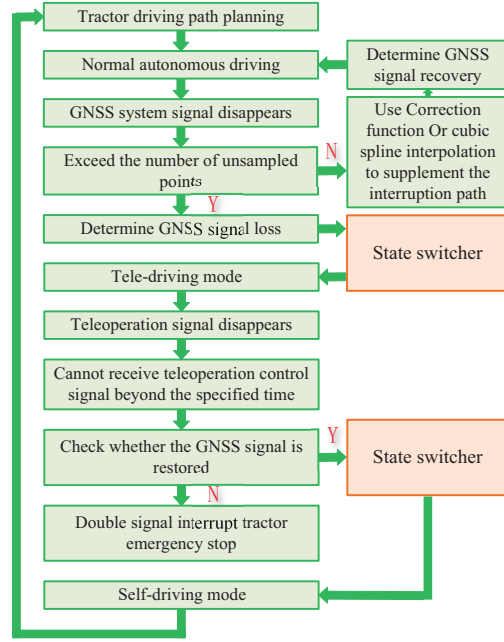


Fig. 4: The step of the tractor switching control.

300) (the maximum delay time λ_1 s was specified above), it can be judged as GNSS signal interruption, which needs to be switched to TD mode. When the number of the signal interruption sampling point is less than n_{max} , the signal is deemed to be recovery which means the SD mode can be continued.

For the TD mode, the maximum interruption time is set as ς s ($\varsigma = 5$). That is to say, if the tractor cannot receive the TD control signal within the specified time, the command signal of TD is deemed to be interrupted. In this case, GNSS signal needs to be reevaluated whether the signal is recovered before the emergency stop. The step of the tractor switching control was given in Fig. 4.

IV. TRACTOR CONTROL METHOD

According to the characteristics of different driving modes, the corresponding control methods and switching control laws were designed to achieve smooth switching between the two driving modes.

A. System control method

Inspired by the existing literature [58]–[60], the unmanned tractor driving switching control method was designed as shown in Fig. 5, whose inputs of state switcher are ρ , B and μ , and the out is the θ . The switch controller and the subsystem controller for corresponding driving mode were designed according to different farmland operation needs and working environments of tractor.

Here, the real-time location information of the unmanned tractor is transmitted from the GNSS system to the central processing unit (The industrial computer placed in the cockpit) via the communication line. Then the central processing unit compares the position of the tractor with that in the desired route to calculate the corresponding correction information,

and transmits it to the corresponding controller in the TD or SD driving mode to realize the closed-loop control tracking of the overall position. And the control state switching command is issued based on Modbus protocol to ensure accuracy and reliability of the switching commands effectively.

B. Tele-driving control of tractor

Considering the tractor as a rigid body nonlinear system [4], not only the complex and changeable farmland operating environment but also the human factor of the operator in the TD mode need to be taken into account. The PID (Proportion Integral Differential) controller plays good effect on the model-free system, which is suitable for TD system with uncertain factors caused by the operator. In view that the adjustment of PID control parameters plays an important role during control, some scholars used heuristic-based coordinate descent algorithm, minimum variance control, and etc. to adjust them and achieve good control effect in their results [61]–[63]. The fuzzy PID control is closer to the thinking and reasoning habit of human beings and can process fuzzy information without relying on the mathematical model of the controlled object [11], [64]–[66]. Therefore, a closed-loop control model between the human and tractor was established in this part based on fuzzy PID controller to achieve a stable control effect of vehicle turning angle.

In this control subsystem, the actual steering angle (θ) information is detected by the encoder and the torque sensor to form a closed-loop position feedback. The fuzzy controller outputs the adjusted parameters such as Proportion, Integral, and Differential to the PID controller. In the controller, the fuzzy linguistic variables are divided into negative big (NB), negative middle (NM), negative small (NS), zero (ZO), positive small (PS), positive middle (PM), and positive big (PB). The error e , the current deviation and the last deviation change ec , the fuzzy subset of the output control parameters are all divided as NB, NM, NS, ZO, PS, PM, PB. The membership functions of them are triangle membership functions, which can be expressed as

$$f(x, a_f, b_f, c_f) = \begin{cases} 0, & x \leq a_f \\ \frac{x - a_f}{b_f - a_f}, & a_f \leq x \leq b_f \\ \frac{c_f - x}{c_f - b_f}, & b_f \leq x \leq c_f \\ 0, & x > c_f \end{cases} \quad (6)$$

Here, the function in Eq. (6) belongs to Type-2 fuzzy set, whose main feature is to fuzzify the membership value of fuzzy set again to improve the ability to deal with uncertainty. After repeated trials, the fuzzy inference rules were given in Appendix E. Fig. 6 was shown the three-dimensional output of fuzzy rules of the control parameters.

The defuzzification method used in this paper is the center of gravity method, whose expression is

$$z_0 = \frac{\sum_{i=0}^n \mu_c(z_i) \cdot z_i}{\sum_{i=0}^n \mu_c(z_i)} \quad (7)$$

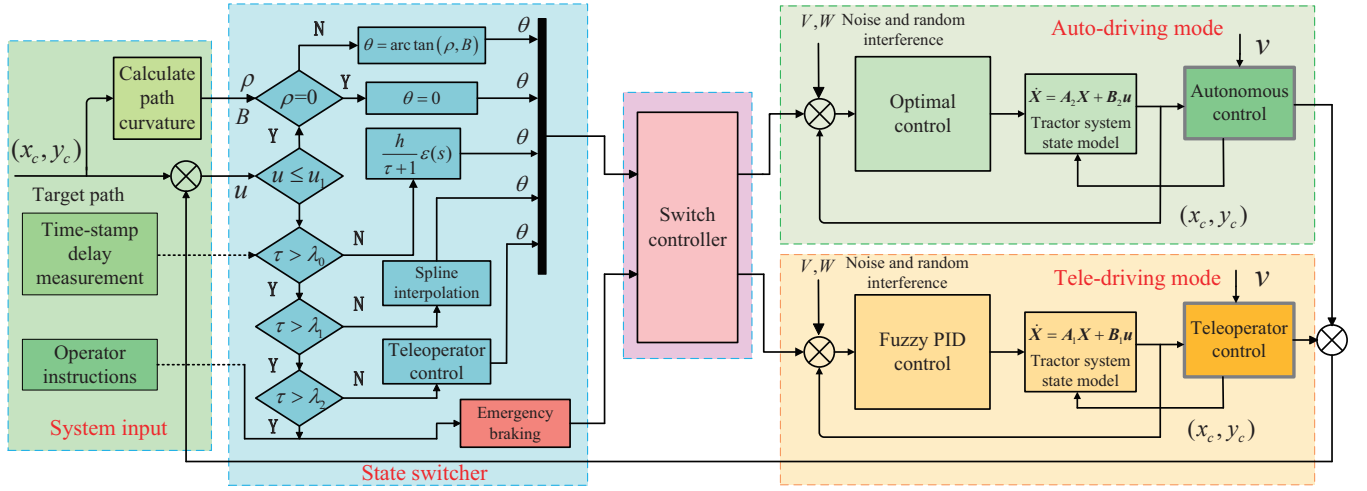
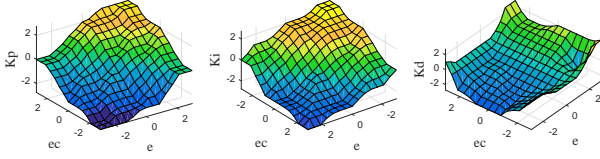
Fig. 5: Diagram of driving switching control method ¹.

Fig. 6: The surface of fuzzy PID control.

C. Self-driving control of tractor

Optimal control is popular in robot motion control, trajectory tracking control, process control, etc., whose essence is to design the suitable control law within the range to make the best performance of the controlled object. Moreover, the technology of information fusion has been used in the tractor SD mode considering the measurement error of the sensor. The stochastic optimal control method was used to design the controller in SD mode. The system model in Eq. (1) is given as

$$\dot{X}(t) = A(t)X(t) + B(t)u(t) + W(t) \quad (8)$$

The measurement equation is

$$Z(t) = H(t)X(t) + V(t) \quad (9)$$

where, the process noise $W(t)$ is not related to the measurement noise $V(t)$, which implies

$$\begin{aligned} E[W(t)] &= 0 & E[V(t)] &= 0 \\ E[V(t)W^T(\bar{t})] &= 0 & (\forall t, \bar{t} = 0, 1, 2, \dots) \end{aligned} \quad (10)$$

Here, the process noise and measurement noise are considered as white noise which obeys the normal distribution.

To take the optimal wheel angle as the control input of the tractor, the linear quadratic regulator (LQR) control was used to realize path tracking in SD mode, which needs to comprehensively consider the information of farmland road, the position deviation and dynamics state of tractor [67], [68]. The performance index can be expressed as

¹The control input in Fig. 5 is the steering angle (θ) of the steering, where satisfied $\theta = f(\delta)$. The function $f(\cdot)$ satisfies the geometric relationship of the designed steering manipulator model.

$$J = \frac{1}{2} \int_0^\infty [X^T(t)QX(t) + u^T(t)Ru(t)]dt \quad (11)$$

where, the first term in the integral is the accumulation of dynamic tracking error in the working process, which represents the total measurement deviation of $X(t)$ from the ideal path; The weighting matrix Q reflects the importance of each component of every state vector, where Q is a symmetric positive definite or semi positive definite moment. The second term in the integral is the control energy consumed by the system in the entire control process, which reflects the cost of control. R is the weighting of each component of the control quantity, and R is a symmetric positive definite matrix. The control integral term is proportional to the amount of control consumed, which means the more consumed, the greater value of the performance index value J .

For the system in Eq. (8), it's controllable because $\text{rank}[B, AB] = 2$, the optimal controller $u(t)$ can be designed as:

$$u(t) = -R^{-1}B^TLX(t) - R^{-1}B^TSW \quad (12)$$

where, $R^{-1}B^TL$ is the state feedback gain matrix; $R^{-1}B^TS$ is the disturbance feedforward gain matrix; L is the positive definite solution of the following Riccati algebraic equation:

$$LA + A^TL - LBR^{-1}B^TL + Q = 0 \quad (13)$$

S can be calculated by the following equation

$$(A^T - LBR^{-1}B^T)S + L = 0 \quad (14)$$

Thus, the optimal control of tractor in SD subsystem was obtained.

D. Dual mode switching control subsystem

1) *The model of switching control subsystem:* Inspired by the switching control in multi-agent theory [69], [70], the following switching control subsystem was designed. Because the system model coefficient matrix varies a lot due to the change of the switching mode, that is, the state matrix and control input matrix are different between TD mode subsystem

and SD mode subsystem. Therefore, the subsystem model of TD mode can be described as

$$\dot{\mathbf{X}} = \mathbf{A}_1 \mathbf{X} + \mathbf{B}_1 \mathbf{u} \quad (15)$$

The subsystem model of SD mode can be described as

$$\dot{\mathbf{X}} = \mathbf{A}_2 \mathbf{X} + \mathbf{B}_2 \mathbf{u} \quad (16)$$

We also define the TD as subsystem 1; the SD as subsystem 2. And the switching subsystem can be described as

$$\dot{\mathbf{X}} = (\mathbf{A}_i + \Delta \mathbf{A}_i) \mathbf{X} + (\mathbf{B}_i + \Delta \mathbf{B}_i) \mathbf{u} \quad (17)$$

where, the calculations of \mathbf{A}_i and \mathbf{B}_i are based on Eq. (1); σ is the switch function which can be expressed as

$$\sigma(\mathbf{X}(t)) = \begin{cases} 1, & \tau > \lambda_1, \mu > \mu_1 \\ 2, & \text{other} \end{cases} \quad (18)$$

Assume that the uncertain term can be decomposed into the following

$$\Delta \mathbf{A}_i = \mathbf{D}_i \mathbf{F}(t) \mathbf{E}_i \quad \Delta \mathbf{B}_i = \mathbf{M}_i \mathbf{F}(t) \mathbf{N}_i \quad (19)$$

where, \mathbf{D}_i , \mathbf{E}_i , \mathbf{M}_i , \mathbf{N}_i are constant-valued matrices with appropriate dimensional, respectively; and $\mathbf{F}(t)$ satisfies

$$\mathbf{F}^T(t) \mathbf{F}(t) \leq \mathbf{I} \quad (20)$$

Among them, the uncertain items can be caused by the measurement errors, changes in input conditions, and abnormal operations of components such as sensors and actuators. The uncertain factors here only represent the uncertainty within a certain range of errors, which can also be regarded as the noise in the control. After the noise was added to the system model, the asymptotic stability of the closed-loop system under all possible failures of sensors and actuators can be ensured.

Lemma 1: [71] For any suitable dimensional matrix \mathbf{X} , \mathbf{Y} and constant $\alpha > 0$, we have

$$\mathbf{X}^T \mathbf{Y} + \mathbf{Y}^T \mathbf{X} \leq \alpha \mathbf{X}^T \mathbf{X} + \alpha^{-1} \mathbf{Y}^T \mathbf{Y} \quad (21)$$

2) *The switching control law of tractor:* Let \mathbf{P} be a symmetric positive definite matrixes of order n , and define the following p sets

$$\Omega_i = \{\mathbf{X} \in \mathbb{R}^n | \mathbf{Z}_i < 0\} \quad (22)$$

where

$$\begin{aligned} \mathbf{Z}_i = & \mathbf{X}^T (\mathbf{A}_i^T \mathbf{P} + \mathbf{P} \mathbf{A}_i - \mathbf{P} \mathbf{B}_i \mathbf{B}_i^T \mathbf{P} + \varepsilon \mathbf{E}_i^T \mathbf{E}_i \\ & + \varepsilon^{-1} \mathbf{P} \mathbf{D}_i \mathbf{D}_i^T \mathbf{P} + 0.25 \gamma \mathbf{P} \mathbf{B}_i \mathbf{N}_i^T \mathbf{N}_i \mathbf{B}_i^T \mathbf{P} \\ & + \gamma^{-1} \mathbf{P} \mathbf{M}_i \mathbf{M}_i^T \mathbf{P}) \mathbf{X} \quad (i = 1, 2, \dots, p) \end{aligned} \quad (23)$$

Lemma 2: [72] If a matrix can be divided into small matrices \mathbf{U}_1 , \mathbf{U}_2 , \mathbf{U}_3 , where \mathbf{U}_2 is an invertible matrix, the following relationship is existed

$$\begin{bmatrix} \mathbf{U}_1 & \mathbf{U}_2^T \\ \mathbf{U}_2 & \mathbf{U}_3 \end{bmatrix} < 0 \quad (24)$$

Then there must be

$$\mathbf{U}_1 - \mathbf{U}_2^T \mathbf{U}_3^{-1} \mathbf{U}_2 < 0 \quad (25)$$

Theorem 1: If there is a symmetric positive definite matrix \mathbf{P} and the normal numbers β_i , ε , γ , such that the convex combination of \mathbf{Z}_i satisfies $\sum_{i=1}^m \beta_i \mathbf{Z}_i < 0$ ($\sum_{i=1}^m \beta_i = 1$), then a controller \mathbf{u} ($\mathbf{u} = \mathbf{K}_i \mathbf{X}$, where $\mathbf{K}_i = -\frac{1}{2} \mathbf{B}_i^T \mathbf{P}$) and a switching strategy $\sigma(\mathbf{X}(t))$

are existed, which can make the uncertain switching system in Eq. (17) stable.

The control input is as following

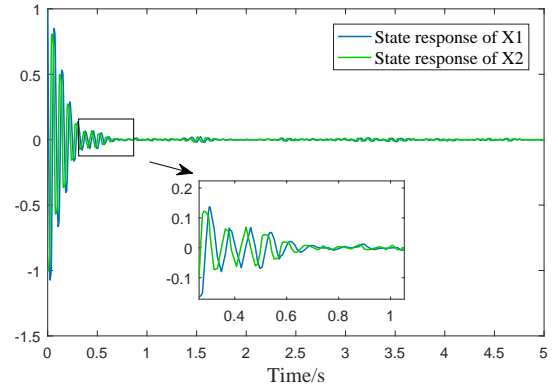
$$\mathbf{u} = \mathbf{K}_i \mathbf{X} \quad (26)$$

and the switching strategy can be expressed as

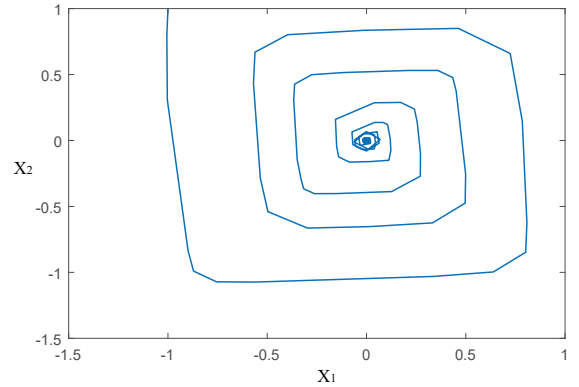
$$\sigma(\mathbf{X}(t)) = \arg \left\{ \min_{ij} \mathbf{Z}_{ij}(\mathbf{X}) < 0 \right\} \quad (27)$$

The proof of the main theorem was given in Appendix D.

3) *Simulation of switching control law:* In this section, we substitute the parameters to verify the stability of the switching system. According to Theorem 1, the premise of system stability is the existence of a symmetric positive definite matrix \mathbf{P} , where the specific method of \mathbf{P} is solved by lemma 2. First, let



(a) State response curve



(b) State trajectory

Fig. 7: The simulation result of switch control.

$$\begin{aligned} \mathbf{H}_i = & \mathbf{A}_i^T \mathbf{P} + \mathbf{P} \mathbf{A}_i - \mathbf{P} \mathbf{B}_i \mathbf{B}_i^T \mathbf{P} + \varepsilon \mathbf{E}_i^T \mathbf{E}_i \\ & + \varepsilon^{-1} \mathbf{P} \mathbf{D}_i \mathbf{D}_i^T \mathbf{P} + 0.25 \gamma \mathbf{P} \mathbf{B}_i \mathbf{N}_i^T \mathbf{N}_i \mathbf{B}_i^T \mathbf{P} \\ & + \gamma^{-1} \mathbf{P} \mathbf{M}_i \mathbf{M}_i^T \mathbf{P} \quad (i = 1, 2) \end{aligned} \quad (28)$$

Then, we calculate $\sum_{i=1}^m \mathbf{H}_i < 0$ ($m = 2$) based on linear matrix inequality. Here, it can be equivalent to solving

$$\begin{bmatrix} \mathbf{Q} \bar{\mathbf{A}}^T + \bar{\mathbf{A}} \mathbf{Q} + \mathbf{R} & \mathbf{X} \\ \mathbf{X}^T & \mathbf{M} \end{bmatrix} < 0 \quad (29)$$



Fig. 8: The overall layout of driving robot.

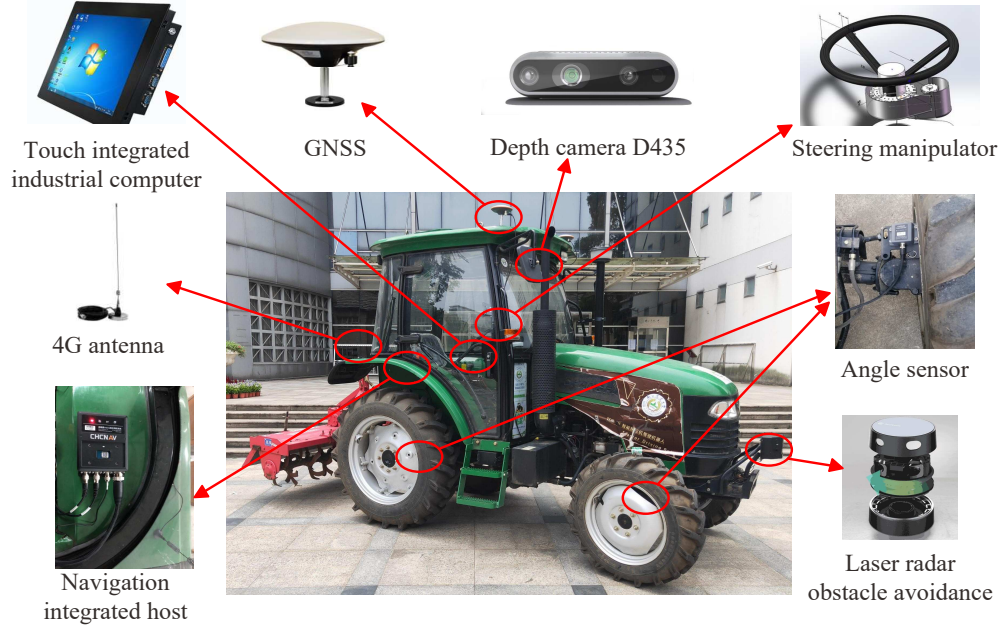


Fig. 9: The design of unmanned driving tractor.

where, $Q = P^{-1}$, $\bar{A} = \sum_{i=1}^m \beta_i A_i$, $\bar{\beta}_i = \beta_i^{-1} \varepsilon^{-1}$, and

$$R = \sum_{i=1}^m \beta_i [-B_i B_i^T + \beta_i \bar{\beta}_i D_i D_i^T + 0.25 \gamma B_i N_i^T N_i B_i^T + \gamma^{-1} M_i M_i^T] \quad (30)$$

$$X = [Q E_1^T, \dots, Q E_m^T] \quad (31)$$

$$M = \text{diag} \{-\bar{\beta}_1 I, \dots, -\bar{\beta}_m I\} \quad (32)$$

The positive definite matrix Q can be obtained by solving the Eq. (29) based on the linear matrix inequality (LMI) method. Therefore, the symmetric positive definite matrix P can be obtained as well, which can be expressed as

$$P = \begin{bmatrix} 65.3106 & 57.9485 \\ 57.9485 & 231.2671 \end{bmatrix} \quad (\varepsilon = 1.21351 \quad \gamma = 1) \quad (33)$$

According to *Theorem 1*, the switch system designed is asymptotically stable. The simulation result was shown in Fig.

7, which verified that the designed switching control law is correct and effective.

V. EXPERIMENT

A. Experiment platform

The tractor driving robot in this article was installed on a tractor of model CFD504A (Changfa Co. China) to realize the ordinary tractor intelligent upgrade rapidly and nondestructively. The robot is composed of control manipulators/legs (shift manipulator, steering manipulator, and pedal mechanical leg), sensing units, industrial control computer, electric control units, hydraulic control units, and various power output units, which uses a combination of motor drive and hydraulic drive to realize precise control of driving robot. The overall layout of driving robot was shown in Fig. 8. The main parameters of the tractor driving platform used in the experiment were listed in the Appendix F including the body performance parameters of the tractor, the main relevant component parameters of measurement and control subsystem. The navigation system

for SD consists of GNSS and Delta-III lidar units to achieve high precision navigation by using multi-sensor data fusion technology to combine satellite positioning information, inertial information and lidar information. The components of unmanned driving tractor were shown in Fig. 9.

B. Experiment procedure

1) *Design of experiment procedure:* To evaluate the safety and reliability of the proposed control method, the unmanned driving tractor was set to work around the Pukou campus of Nanjing Agricultural University under supervision. The testing needs to pass through different road conditions such as flat ground, mud, slopes, and tree-lined roads during the experiments. The driving route starts from point A and ends at point H after a counterclockwise circle around the campus. The tractor maintains a constant speed of 12 km/h throughout the entire journey (Unlike the vehicles travel in the road, an unmanned tractor usually works at a constant low speed during the same operation task to ensure the agricultural operation quality). The total testing distance is about 1.80 km. Short time failure of autonomous navigation will occur because of GNSS signal lost on some sections of the road caused by the shade of trees. The road conditions of each section were shown in Table I.

TABLE I: The road conditions of each section.

Path section	Road conditions	Distance
AB	Flat road and some areas blocked by trees	0.4 km
BC	Uphill road, partly blocked by trees	0.4 km
CD	Uphill, relatively open, small part blocked	0.1 km
DE	Uphill, open area	0.3 km
EF	Uphill road, heavily blocked by trees	0.2 km
FG	Relatively open, partially blocked by trees	0.1 km
GH	Flat road and open area	0.3 km

2) *Experiment procedure:* To visualize the experimental results, the GNSS data was imported into Google Earth to record the experimental trajectory, as shown in Fig. 10.



Fig. 10: Tacking trajectory.

The actual working conditions of each planned path were given in Table II. Results demonstrate that the unmanned tractor based on dual-mode control has sensitive accident

handling ability and high reliability, therefore, it also has practical applicability and maneuverability.

TABLE II: Working conditions of each planned path.

Path section	GNSS signal	Teleoperation signal	Whether interpolate	Control mode
AB	—	✓	✓ (Point A)	SD
BC	✓	✓	×	SD
CD	×	✓	✓ (Point B)	TD
DE	✓	✓	×	SD
EF	—	✓	✓ (Point C)	SD
FG	✓	✓	×	SD
GH	✓	✓	×	SD

C. Results Analysis

1) *Interpolation effect under missing path:* Points a, b, and c are the automatic interpolation points when the GNSS signal is weak or lost during the experiment. The specific results were shown in Table III.

TABLE III: Conditions of interpolations points.

Point	Failure distance	Maximum error	Minimum error	Average error	Whether switch
a	1.50 m	0.14 m	0.05 m	0.095 m	NO
b	45.0 m	0.17 m	0.11 m	0.14 m	YES
c	1.0 m	0.12 m	0.08 m	0.10 m	NO

Experimental results show that using the cubic spline interpolation method to supplement the path of the tractor driving trajectory can restore the expected trajectory with high degree of fitness to avoid path deviation caused by the lack of navigation information.

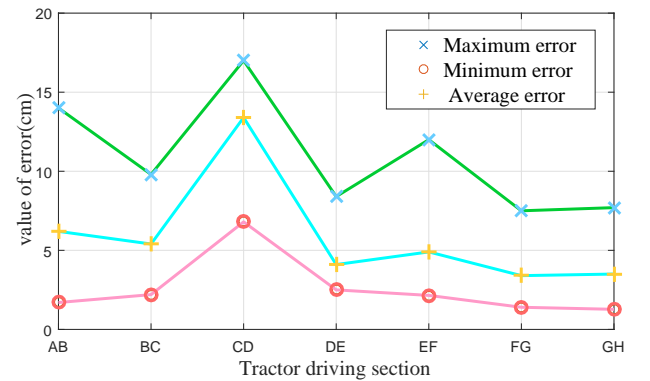


Fig. 11: The error data of each driving section.

2) *System error:* Position error of each travel section was obtained according to the experimental data as shown in Fig.11. As expected, the system can switch the control mode in real time based on the logic rules to fulfill the requirements of the preset farmland farming path. Further, even in the CD road section where the navigation signal is seriously lost due to the influence of communication, the maximum tracking error, minimum tracking error and average tracking error of the whole section are not more than 17.00 cm, 1.27 cm, 5.62 cm, respectively, which can meet the actual operation requirements of the agricultural machinery.

3) *Comparison of experimental results:* Keeping the experimental trajectory the same, the control conditions were changed for comparing the tracking error under different control modes (Fig. 12). Here, the maximum error indicates the measurement error of the sensor in the case of absolutely failure.

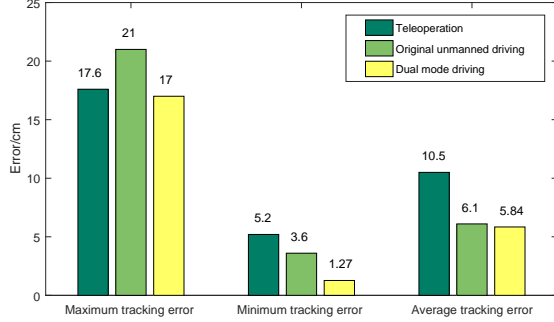


Fig. 12: Error comparison of different control methods.

As shown in Fig. 12, the dual-mode driving control algorithm proposed in this paper can reduce the costs of labor and improve the overall control stability of the system compared with that of only TD control. The maximum tracking error, minimum tracking error and average tracking error were reduced by 0.60 cm, 3.93 cm, 4.66 cm, respectively, and the overall average control accuracy of the system was increased by approximately 20%.

Likewise, the results of only SD control were compared with those of the dual-mode driving control, which show that the dual-mode control algorithm can not only make up for the low accuracy of ordinary GPS (Global Positioning System) navigation in terms of hardware, but also reduce the maximum tracking error, minimum tracking error and average tracking error with 4.00 cm, 2.33 cm, 0.26 cm, respectively. It improves the overall average control accuracy by about 15%.

4) *The speed of the tractor:* The speed curve of the tractor in the experiment, shown in Fig. 13, indicates that the tractor with dual-mode driving control can move forward at a relatively stable speed during the experiment with the average speed and the maximum speed at 12.491 km/h and 14.430 km/h, respectively.

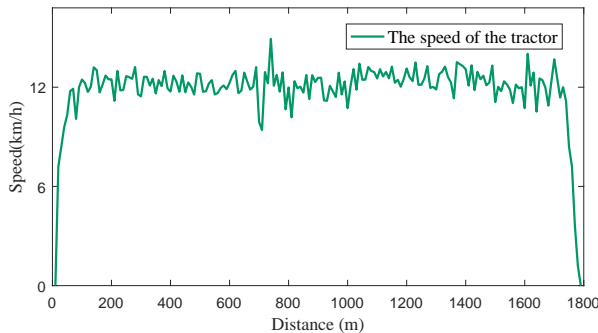


Fig. 13: The speed of the tractor.

It is worth noting that the tractor speed in SD control mode

changes steadily, but that in TD control mode fluctuates relatively high influenced by the operator, specifically at $x = 800$ m (At this time, the driving mode is TD).

D. Comparison of tractor driving

TABLE IV: Comparison of tractor driving performance.

Comparison	Reference	Application	Experimental data	
			Tracking error / mm	
			Maximum	Average
TD	This Paper	Tractor	210	105
	[30]	Tractor	-	-
	[31]	Tractor	261	215
SD	This Paper	Tractor	210	61.0
	[13]	Tractor	-	-
	[14]	Surface Vehicle	1450	780
	[27]	Tractor	-	400
	[29]	Vehicle	370	103
	[73]	Tractor	272	68
Dual-mode	[74]	Tractor	-	39
	This Paper	Tractor	170	58.4
	[39]	Tractor	140	60
	[43]	Tractor	283	87.8
	[75]	Vehicle	-	-

To verify the advantages of the proposed method, the comparison results between the proposed solution in the paper with the single-mode driving and dual-mode driving were shown in Table IV, which indicates that the tractor control accuracy of TD method is largely influenced by many factors such as driver experience, road condition and environment, manipulation type and signal transmission, et.al. It's hard to show the advantages of the proposed method in this paper through simple trajectory error comparison. Therefore, it is only necessary to ensure that the tractor under TD mode can complete the farmland operation and meet the farmland operation requirements.

In this section, the comparison of tractor trajectory tracking error between different SD methods was carried out. [13] is a review of unmanned tractor, which lists the operating performance of 13 typical unmanned tractors. On the basis of the literature [13] and the Table IV, the tracking accuracy based on the subsystem of SD mode designed in this paper is better than the most existing unmanned tractor, moreover, with higher safety and reliability. A man-machine driving method presented in [39] can improve the control accuracy of a tractor but increase the cost burden at the same time because two tractors are required to deal with the work. The research ideas of [43] and [75] are similar to this paper. However, the driving accuracy in [43] is lower than that of this paper, which may be caused by the limitation of sensing accuracy and control method; A multimode driving application was realized in [75] but the theoretical methods and detailed experimental data were not given. In summary, the dual-mode switching control method proposed in this paper is superior to the existing tractor control methods not only in precision but also in security and reliability.

VI. CONCLUSION

A dual-mode switching control method with high security and reliability was proposed in this paper, which is composed

of the controllers of different driving modes to integrate the advantages of both autonomous driving and remote driving. Then, the experiments were carried out for evaluating the performance of the strategy which results demonstrate that the driving system can respond to the control commands in time and complete the agricultural operations with high precision using the proposed dual-mode switching control method. In addition, it can not only compensate for the instability of the SD mode, but also frees manpower from the point-to-point TD mode, which greatly improves work reliability and safety. Moreover, the control accuracy of the method proposed in this paper is obviously better than that of the existing literature, and the safety performance is also extremely improved. In conclusion, the method in this paper has a good application prospect and provides reliable theoretical support and practical application for the unmanned farmland and intelligent agriculture.

In the future, the cooperative operation of multiple unmanned tractors will be researched based on the system in this paper, which can further improve the efficiency of farmland planting.

REFERENCES

- [1] M. Pathan, N. Patel, H. Yagnik, and M. Shah, "Artificial cognition for applications in smart agriculture: A comprehensive review," *Artificial Intelligence in Agriculture*, vol. 4, pp. 81–95, 2020.
- [2] M. Bacco, P. Barsocchi, E. Ferro, A. Gotta, and M. Ruggeri, "The Digitisation of Agriculture: A Survey of Research Activities on Smart Farming," *Array*, vol. 3–4, 2019.
- [3] X. Yang et al., "A Survey on Smart Agriculture: Development Modes, Technologies, and Security and Privacy Challenges," *IEEE/CAA J. Autom. Sin.*, vol. 8, no. 2, pp. 273–302, 2021.
- [4] K. Alipour, A. B. Robat, and B. Tarvirdizadeh, "Dynamics modeling and sliding mode control of tractor-trailer wheeled mobile robots subject to wheels slip," *Mech. Mach. Theory*, vol. 138, pp. 16–37, 2019.
- [5] Y. Ding, L. Wang, Y. Li, and D. Li, "Model predictive control and its application in agriculture: A review," *Comput. Electron. Agric.*, vol. 151, no. December 2017, pp. 104–117, 2018.
- [6] P. M. Kebria, A. Khosravi, S. M. Salaken, and S. Nahavandi, "Deep imitation learning for autonomous vehicles based on convolutional neural networks," *IEEE/CAA J. Autom. Sin.*, vol. 7, no. 1, pp. 82–95, 2020.
- [7] Q. Zhou, Y. Zhang, Z. Li, J. Li, H. Xu, and O. Olatunbosun, "Cyber-Physical Energy-Saving Control for Hybrid Aircraft-Towing Tractor Based on Online Swarm Intelligent Programming," *IEEE Trans. Ind. Informatics*, vol. 14, no. 9, pp. 4149–4158, 2018.
- [8] H. Guo et al., "Hazard-evaluation-oriented moving horizon parallel steering control for driver-automation collaboration during automated driving," *IEEE/CAA J. Autom. Sin.*, vol. 5, no. 6, pp. 1062–1073, 2018.
- [9] I. Eski and Z. A. Kus, "Control of unmanned agricultural vehicles using neural network-based control system," *Neural Comput. Appl.*, vol. 31, pp. 583–595, 2019.
- [10] Y. Deng, T. Zhang, G. Lou, X. Zheng, J. Jin, and Q. L. Han, "Deep Learning-Based Autonomous Driving Systems: A Survey of Attacks and Defenses," *IEEE Trans. Ind. Informatics*, vol. 3203, no. c, pp. 1–16, 2021.
- [11] X. Zhao, H. Mo, K. Yan, and L. Li, "Type-2 fuzzy control for driving state and behavioral decisions of unmanned vehicle," *IEEE/CAA J. Autom. Sin.*, vol. 7, no. 1, pp. 178–186, 2020.
- [12] S. Bonadies and S. A. Gadsden, "An overview of autonomous crop row navigation strategies for unmanned ground vehicles," *Eng. Agric. Environ. Food*, vol. 12, no. 1, pp. 24–31, 2019.
- [13] A. Roshanianfard, N. Noguchi, H. Okamoto, and K. Ishii, "A review of autonomous agricultural vehicles (The experience of Hokkaido University)," *J. Terramechanics*, vol. 91, pp. 155–183, 2020.
- [14] Y. Liu and N. Noguchi, "Development of an unmanned surface vehicle for autonomous navigation in a paddy field," *Eng. Agric. Environ. Food*, vol. 9, no. 1, pp. 21–26, 2016.
- [15] Y. Shang, "Subgraph Robustness of Complex Networks under Attacks," *IEEE Trans. Syst. Man, Cybern. Syst.*, vol. 49, no. 4, pp. 821–832, 2019.
- [16] Y. Yuan, Y. Wang, and L. Guo, "Force reflecting control for bilateral teleoperation system under time-varying delays," *IEEE Trans. Ind. Informatics*, vol. 15, no. 2, pp. 1162–1172, 2019.
- [17] S. Hangai and T. Nozaki, "Haptic Data Prediction and Extrapolation for Communication Traffic Reduction of Four-Channel Bilateral Control System," *IEEE Trans. Ind. Informatics*, vol. 17, no. 4, pp. 2611–2620, 2021.
- [18] Z. Zhao, J. Yang, S. Li, and W. H. Chen, "Composite nonlinear bilateral control for teleoperation systems with external disturbances," *IEEE/CAA J. Autom. Sin.*, vol. 6, no. 5, pp. 1220–1229, 2019.
- [19] U. Edet and D. Mann, "Visual information requirements for remotely supervised autonomous agricultural machines," *Appl. Sci.*, vol. 10, no. 8, 2020.
- [20] Y. Chen, B. Zhang, J. Zhou, and K. Wang, "Real-time 3D unstructured environment reconstruction utilizing VR and Kinect-based immersive teleoperation for agricultural field robots," *Comput. Electron. Agric.*, vol. 175, no. April, p. 105579, 2020.
- [21] X. K. Xu, X. M. Li, and R. H. Zhang, "Remote Configurable Image Acquisition Lifting Robot for Smart Agriculture," *Proc. 2019 IEEE 4th Adv. Inf. Technol. Electron. Autom. Control Conf. IAEAC 2019*, pp. 1545–1548, 2019.
- [22] Z. Lu and J. C. F. de Winter, "A Review and Framework of Control Authority Transitions in Automated Driving," *Procedia Manuf.*, vol. 3, no. Ahfe, pp. 2510–2517, 2015.
- [23] D. H. Kim, C. H. Choi, and Y. J. Kim, "Analysis of driving performance evaluation for an unmanned tractor," *IFAC-PapersOnLine*, vol. 51, no. 17, pp. 227–231, 2018.
- [24] C. Huang, F. Naghdy, H. Du, and H. Huang, "Shared control of highly automated vehicles using steer-by-wire systems," *IEEE/CAA J. Autom. Sin.*, vol. 6, no. 2, pp. 410–423, 2019.
- [25] X. Zhou and J. Zhou, "Data-Driven Driving State Control for Unmanned Agricultural Logistics Vehicle," *IEEE Access*, vol. 8, pp. 65530–65543, 2020.
- [26] G. Chen and W. Zhang, "Hierarchical Coordinated Control Method for Unmanned Robot Applied to Automotive Test," *IEEE Trans. Ind. Electron.*, vol. 63, no. 2, pp. 1039–1051, 2016.
- [27] A. S. Matveev, M. Hoy, J. Katupitiya, and A. V. Savkin, "Nonlinear sliding mode control of an unmanned agricultural tractor in the presence of sliding and control saturation," *Rob. Auton. Syst.*, vol. 61, no. 9, pp. 973–987, 2013.
- [28] W. Upaphai, P. Bunyanichakul, and M. Janthong, "Design of self-tuning fuzzy PID controllers for position tracking control of autonomous agricultural tractor," *Pertanika J. Sci. Technol.*, vol. 27, no. 1, pp. 263–280, 2019.
- [29] E. Kayacan, W. Saeys, H. Ramon, C. Belta, and J. M. Peschel, "Experimental Validation of Linear and Nonlinear MPC on an Articulated Unmanned Ground Vehicle," *IEEE/ASME Trans. Mechatronics*, vol. 23, no. 5, pp. 2023–2033, 2018.
- [30] E. D. C. C. Penido, M. Martins, H. C. Fernandes, P. B. Monteiro, and P. R. Cecon, "Development and evaluation of a remotely controlled and monitored self-propelled sprayer in tomato crops," *Rev. Cienc. Agron.*, vol. 50, no. 1, pp. 8–17, 2019.
- [31] Y. J. Wang, F. Z. Yang, G. T. Pan, H. Y. Liu, Z. J. Liu, and J. Q. Zhang, "Design and testing of a small remote-control hillside tractor," *Trans. ASABE*, vol. 57, no. 2, pp. 363–370, 2014.
- [32] T. J. Lutz and G. T. Homce, "Remote control of an agricultural tractor in SAE field upset tests," *Int. J. Veh. Des.*, vol. 34, no. 3, pp. 286–296, 2004.
- [33] D. O. Gonzalez, B. M. Gorri, I. I. Berrocal, A. M. Morales, G. A. Salcedo, and B. M. Hernandez, "Development and assessment of a tractor driving simulator with immersive virtual reality for training to avoid occupational hazards," *Comput. Electron. Agric.*, vol. 143, no. September, pp. 111–118, 2017.
- [34] F. Xu, X. Liu, W. Chen, and C. Zhou, "Dynamic Switch Control of Steering Modes for Four Wheel Independent Steering Rescue Vehicle," *IEEE Access*, vol. 7, no. 3, pp. 135595–135605, 2019.
- [35] H. Han, H. Liu, and J. Qiao, "Knowledge-Data-Driven Flexible Switching Control for Wastewater Treatment Process," *IEEE Trans. Control Syst. Technol.*, pp. 1–14, 2021.
- [36] C. Liu, G. Wen, Z. Zhao, and R. Sedaghati, "Neural-Network-Based Sliding-Mode Control of an Uncertain Robot Using Dynamic Model Approximated Switching Gain," *IEEE Trans. Cybern.*, vol. 51, no. 5, pp. 2339–2346, 2021.
- [37] D. Yang, G. Zong, and S.-F. Su, " H_∞ Tracking Control of Uncertain Markovian Hybrid Switching Systems: A Fuzzy Switching Dynamic Adaptive Control Approach," *IEEE Trans. Cybern.*, pp. 1–12, 2020.

- [38] W. Wang et al., "Decision-making in driver-automation shared control: A review and perspectives," *IEEE/CAA J. Autom. Sin.*, vol. 7, no. 5, pp. 1289–1307, 2020.
- [39] C. Zhang, L. Yang, and N. Noguchi, "Development of a robot tractor controlled by a human-driven tractor system," *Eng. Agric. Environ. Food*, vol. 8, no. 1, pp. 7–12, 2015.
- [40] J. Wang, L. Zhang, D. Zhang, and K. Li, "An adaptive longitudinal driving assistance system based on driver characteristics," *IEEE Trans. Intell. Transp. Syst.*, vol. 14, no. 1, pp. 1–12, 2013.
- [41] J. Huang, Y. Chen, X. Peng, L. Hu, and D. Cao, "Study on the driving style adaptive vehicle longitudinal control strategy," *IEEE/CAA J. Autom. Sin.*, vol. 7, no. 4, pp. 1107–1115, 2020.
- [42] B. Bashiri and D. D. Mann, "Automation and the situation awareness of drivers in agricultural semi-autonomous vehicles," *Biosyst. Eng.*, vol. 124, pp. 8–15, 2014.
- [43] A. Stentz, C. Dima, C. Wellington, H. Herman, and D. Stager, "A system for semi-autonomous tractor operations," *Auton. Robots*, vol. 13, no. 1, pp. 87–104, 2002.
- [44] S. Ma, T. Zanma, and M. Ishida, "Automatic driving system using identification of switched systems with unknown switch points," *IEEJ Trans. Electr. Electron. Eng.*, vol. 1, no. 4, pp. 426–437, 2006.
- [45] M. Karkee and B. L. Steward, "Study of the open and closed loop characteristics of a tractor and a single axle towed implement system," *J. Terramechanics*, vol. 47, no. 6, pp. 379–393, 2010.
- [46] H. Wang and N. Noguchi, "Real-time states estimation of a farm tractor using dynamic mode decomposition," *GPS Solut.*, vol. 25, no. 1, 2021.
- [47] Z. Liu, M. Yue, L. Guo, and Y. Zhang, "Trajectory planning and robust tracking control for a class of active articulated tractor-trailer vehicle with on-axle structure," *Eur. J. Control*, vol. 54, pp. 87–98, 2020.
- [48] J. Cai, H. Jiang, L. Chen, J. Liu, Y. Cai, and J. Wang, "Implementation and Development of a Trajectory Tracking Control System for Intelligent Vehicle," *J. Intell. Robot. Syst. Theory Appl.*, vol. 94, no. 1, pp. 251–264, 2019.
- [49] M. L. Cummings, "Adaptation of Human Licensing Examinations to the Certification of Autonomous Systems," *Safe, Auton. Intell. Veh.*, pp. 145–162, 2019.
- [50] X. Han, H. J. Kim, C. W. Jeon, H. C. Moon, J. H. Kim, and S. Y. Yi, "Application of a 3D tractor-driving simulator for slip estimation-based path-tracking control of auto-guided tillage operation," *Biosyst. Eng.*, vol. 178, pp. 70–85, 2019.
- [51] J. Lowenberg-DeBoer et al., "Lessons to be learned in adoption of autonomous equipment for field crops," *Appl. Econ. Perspect. Policy*, no. June, pp. 1–17, 2021.
- [52] T. Bakker, K. van Asselt, J. Bontsema, J. Miller, and G. van Straten, "Autonomous navigation using a robot platform in a sugar beet field," *Biosyst. Eng.*, vol. 109, no. 4, pp. 357–368, 2011.
- [53] B. Cai, L. Zhang, and Y. Shi, "Observed-Mode-Dependent State Estimation of Hidden Semi-Markov Jump Linear Systems," *IEEE Trans. Automat. Contr.*, vol. 65, no. 1, pp. 442–449, 2020.
- [54] Z. G. Wu, S. Dong, H. Su and C. Li, "Asynchronous Dissipative Control for Fuzzy Markov Jump Systems," *IEEE Trans. Cybern.*, vol. 48, no. 8, pp. 2426–2436, 2018.
- [55] M. Shen, J. H. Park, and D. Ye, "A Separated Approach to Control of Markov Jump Nonlinear Systems with General Transition Probabilities," *IEEE Trans. Cybern.*, vol. 46, no. 9, pp. 2010–2018, 2016.
- [56] S. Dong, H. Zhu, S. Zhong, K. Shi, and Y. Liu, "New study on fixed-time synchronization control of delayed inertial memristive neural networks," *Appl. Math. Comput.*, vol. 399, 2021.
- [57] L. Hua, H. Zhu, K. Shi, S. Zhong, Y. Tang, and Y. Liu, "Novel Finite-Time Reliable Control Design for Memristor-Based Inertial Neural Networks with Mixed Time-Varying Delays," *IEEE Trans. Circuits Syst.*, vol. 68, no. 4, pp. 1599–1609, 2021.
- [58] G. Xu et al., "Path following control of tractor with an electro-hydraulic coupling steering system: Layered multi-loop robust control architecture," *Biosyst. Eng.*, vol. 209, pp. 282–299, 2021.
- [59] Y. Shang, "Group consensus of multi-agent systems in directed networks with noises and time delays," *Int. J. Syst. Sci.*, vol. 46, no. 14, pp. 2481–2492, 2015.
- [60] Y. Shang, "Resilient Consensus for Expressed and Private Opinions," *IEEE Trans. Cybern.*, vol. 51, no. 1, pp. 318–331, 2021.
- [61] A. H. Khan, Z. Shao, S. Li, Q. Wang, and N. Guan, "Which is the best PID variant for pneumatic soft robots? an experimental study," *IEEE/CAA J. Autom. Sin.*, vol. 7, no. 2, pp. 451–460, 2020.
- [62] S. K. Pradhan and B. Subudhi, "Position control of a flexible manipulator using a new nonlinear self-Tuning PID controller," *IEEE/CAA J. Autom. Sin.*, vol. 7, no. 1, pp. 136–149, 2020.
- [63] A. Behera, T. K. Panigrahi, P. K. Ray, and A. K. Sahoo, "A novel cascaded PID controller for automatic generation control analysis with renewable sources," *IEEE/CAA J. Autom. Sin.*, vol. 6, no. 6, pp. 1438–1451, 2019.
- [64] L. Hu, X. Pan, Z. Tan, and X. Luo, "A Fast Fuzzy Clustering Algorithm for Complex Networks via a Generalized Momentum Method," *IEEE Trans. Fuzzy Syst.*, vol. 14, no. 8, 2021.
- [65] D. Wu, X. Luo, M. Shang, Y. He, G. Wang, and X. Wu, "A Data-Characteristic-Aware Latent Factor Model for Web Services QoS Prediction," *IEEE Trans. Knowl. Data Eng.*, 2020.
- [66] X. Luo, Y. Yuan, S. Chen, N. Zeng, and Z. Wang, "Position-Transitional Particle Swarm Optimization-incorporated Latent Factor Analysis," *IEEE Trans. Knowl. Data Eng.*, 2020.
- [67] B. Li, T. Acarman, Y. Zhang, L. Zhang, C. Yaman, and Q. Kong, "Tractor-Trailer Vehicle Trajectory Planning in Narrow Environments with a Progressively Constrained Optimal Control Approach," *IEEE Trans. Intell. Veh.*, vol. 5, no. 3, pp. 414–425, 2019.
- [68] J. Tian, Q. Zeng, P. Wang, and X. Wang, "Active steering control based on preview theory for articulated heavy vehicles," *PLoS One*, vol. 16, no. 5 May, pp. 1–17, 2021.
- [69] Y. Shang, "Resilient consensus of switched multi-agent systems," *Syst. Control Lett.*, vol. 122, pp. 12–18, 2018.
- [70] Y. Shang, "Interval consensus of switched multiagent systems," *Int. J. Syst. Sci.*, 2021.
- [71] J. M. Collado and I. R. Petersen, "A stabilization algorithm for a class of uncertain linear systems," *Syst. Control Lett.*, vol. 11, no. 1, p. 83, 1988.
- [72] Y. Chang, G. Zhai, B. Fu, and L. Xiong, "Quadratic stabilization of switched uncertain linear systems: A convex combination approach," *IEEE/CAA J. Autom. Sin.*, vol. 6, no. 5, pp. 1116–1126, 2019.
- [73] Y. Li, Q. Cao, and F. Liu, "Design of control system for driverless tractor," *MATEC Web Conf.*, vol. 309, p. 04001, 2020.
- [74] E. Mousavinejad, X. Ge, Q. L. Han, T. J. Lim, and L. Vlacic, "An Ellipsoidal Set-Membership Approach to Distributed Joint State and Sensor Fault Estimation of Autonomous Ground Vehicles," *IEEE/CAA J. Autom. Sin.*, vol. 8, no. 6, pp. 1107–1118, 2021.
- [75] Y. Zhang, K. Li, and W. Li, "Design and Realization of Unmanned Multi-mode Collaborative Intelligent Driving System," *SID Symp. Dig. Tech. Pap.*, vol. 51, no. S1, pp. 201–204, 2020.



Wei Lu (Member, IEEE) received the master degree in measurement technology & instrument and Ph.D. degree in instrument science & technology from Southeast University, China, in 2005 and 2012 respectively. He became a Member of IEEE in 2017, a Member of ASABE in 2017, a Director of Jiangsu Province Instrument and Control Society in China in 2015, a Director of Jiangsu Province Automatics Society in China in 2016.

He was an Assistant Professor in Nanjing Agricultural University from 2012 to 2014, and has been an Associate Professor since 2015. He was also a visiting scholar in Michigan State University during 2016 to 2017. His current research interests include intelligent robotics and advanced non-destructive detection technology in agriculture.



Jiacheng Li was born in Xining City, Qinghai Province, China, in 1997. He received the B.S. degree in automation from Nanjing Agricultural University, Nanjing, China, in 2020.

He is currently pursuing the M.S. degree with the Unmanned system Research Institute, Northwestern Polytechnical University, Xian, China. His current research interests include teleoperation control, unmanned driving robot of tractor, and collision avoidance control of cooperative UAVs.



Huanhuan Qin was born in Ma'anshan, China, in 1989. He received the B.S. degree in measurement and control technology and instrumentation from Anhui Polytechnic University, Wuhu, China, in 2012, and the Ph.D. degree in instrument science and technology from Southeast University, Nanjing, China, in 2020.

He is currently a lecturer with the College of Artificial Intelligence, Nanjing Agricultural University. His current research interests include intelligent robotics and smart materials for agricultural applications.

ations.



Lei Shu (Senior Member, IEEE) received the B.S. degree in computer science from the South Central University for Nationalities, Wuhan, China, in 2002, the M.S. degree in computer engineering from Kyung Hee University, Seoul, South Korea, in 2005, and the Ph.D. degree from the Digital Enterprise Research Institute, National University of Ireland, Galway, Ireland, in 2010. Until 2012, he was a Specially Assigned Researcher with the Department of Multimedia Engineering, Graduate School of Information Science and Technology, Osaka University, Suita, Japan. He is currently a Distinguished Professor with Nanjing Agricultural University, Nanjing, China, and a Lincoln Professor with the University of Lincoln, Lincoln, U.K., where he is also the Director of the NAU-Lincoln Joint Research Center of Intelligent Engineering. He has published over 400 papers in related conferences, journals, and books in the areas of sensor networks and Internet of Things. His current H-index is 63 and i10-index is 251 in Google Scholar Citation. His current research interests include wireless sensor networks and Internet of Things.

Dr. Shu has also served as a TPC Member for more than 150 conferences, including DCOSS, MASS, ICC, GLOBECOM, ICCCN, WCNC, and ISCC. He has served over 50 various Co-Chair for international conferences/workshops, such as IWCMC, ICC, ISCC, ICNC, Chinacom, especially the Symposium Co-Chair for IWCMC 2012 and ICC 2012, the General Co-Chair for Chinacom 2014, Qshine 2015, Collaboratecom 2017, DependSys 2018, and SCI 2019, and the TPC Chair for InisCom 2015, NCCA 2015, WICON 2016, NCCA 2016, Chinacom 2017, InisCom 2017, WMNC 2017, and NCCA 2018. He has also served on the Editorial Boards, including the IEEE Transactions on Industrial Informatics, IEEE Communications Magazine, IEEE Network Magazine, IEEE Systems Journal, IEEE Access, and IEEE/CCA Journal of Automatica Sinica.



Aiguo Song (Senior Member, IEEE) received the B.S. degree in automatic control and the M.S. degree in measurement and control from the Nanjing University of Aeronautics and Astronautics, Nanjing, China, in 1990 and 1993, respectively, and the Ph.D. degree in measurement and control from Southeast University, Nanjing, in 1996. From 1996 to 1998, he was an Associate Researcher with the Intelligent Information Processing Laboratory, Southeast University.

From 1998 to 2000, he was an Associate Professor with the Department of Instrument Science and Engineering, Southeast University, where he was the Director of the Robot Sensor and Control Laboratory, from 2000 to 2003. From April 2003 to April 2004, he was a Visiting Scientist with the Laboratory for Intelligent Mechanical Systems, Northwestern University, Evanston, IL, USA. He is currently a Professor with the Department of Instrument Science and Engineering, Southeast University. His research interests include haptic display, robot tactile sensor, and tele-rehabilitation robot.

APPENDIX A NOTATION

Notation	Description
α_f	Side slip angle of the front wheels
α_r	Side slip angle of the rear wheels
δ	Wheel deflection angle
\mathbf{I}	Unit matrix
\bar{T}	Sampling period of system
B	Tractor wheelbase
ρ	Path curvature radius
R	Tractor turning radius
y	Curve equation of the predetermined path
y'	First derivatives of y with respect to time t
y''	Second derivatives of y with respect to time t
h	Scale factor
τ	Delay time
$\lambda_0, \lambda_1, \lambda_2$	Limit delay time
μ	Tractor lateral deviation
μ_1	Value of lateral deviation
θ	Steering angle
ξ	Sampling period of GNSS
n_{max}	Limit sampling point
e	Error of steering angle
ec	Deviation change value
a_f	Parameters of triangle function
b_f	Parameters of triangle function
c_f	Parameters of triangle function
z_0	Exact value of the controller output
z_i	Value in the universe of fuzzy control quantity
$\mu_c(z_i)$	Membership value of z
u	Control variable
\mathbf{A}_i	State matrix of the i -th subsystem
\mathbf{B}_i	Control input matrix of the i -th subsystem
$\Delta \mathbf{A}_i$	Uncertain term
$\Delta \mathbf{B}_i$	Uncertain term
σ	Switch function
P	Symmetric positive definite matrix of order n

APPENDIX B MODELING OF THE TRACTOR

According to Assumption 1 and Assumption 2, the dynamic model of the tractor can be established. The tractor dynamic equations are

$$\begin{cases} F_{yf} \cos \delta - F_{xf} \sin \delta + F_{yr} = m(\dot{v}_y + v_x \omega) \\ l_f(F_{yf} \cos \delta - F_{xf} \sin \delta) - l_r F_{yr} = I_z \dot{\omega} \end{cases} \quad (34)$$

where, F_{fy} and F_{yr} represent the lateral force of the front and rear wheels of the tractor, respectively; F_{xf} and F_{xr} represent the longitudinal force of front and rear wheels of tractor, respectively; l_f and l_r represent the distance from the centroid of the tractor to the front and rear axles, respectively; m is the weight of tractor; v_y and v_x represent the transverse and longitudinal speeds of the tractor, respectively; I_z represents the moment of inertia of the tractor relative to the z-axis; ω is the yaw angular velocity of the tractor.

The lateral force of the front and rear wheels of tractor can be calculated by

$$\begin{cases} F_{yf} = 2c_f \alpha_f = 2c_f(\delta - \arctan(\frac{v_y + l_f \omega}{v_x})) \\ F_{yr} = 2c_r \alpha_r = 2c_r \arctan(\frac{l_r \omega - v_y}{v_x}) \end{cases} \quad (35)$$

where, α_f and α_r represent the side slip angle of the front and rear wheels of the tractor, respectively; c_f and c_r represent the

comprehensive cornering stiffness of the front and rear wheels of the tractor, respectively.

According to Assumption 3, Eq. (34) can be rewritten as

$$\begin{cases} F_{yf} + F_{yr} = m(\dot{v}_y + v_x w) \\ l_f F_{yf} - l_r F_{yr} = I_z \dot{w} \end{cases} \quad (36)$$

Eq. (35) can be rewritten as

$$\begin{cases} F_{yf} = 2c_f \alpha_f = 2c_f \left(\delta - \frac{v_y + l_f w}{v_x} \right) \\ F_{yr} = 2c_r \alpha_r = 2c_r \left(\frac{l_r w - v_y}{v_x} \right) \end{cases} \quad (37)$$

Substituting Eq. (37) into Eq. (36), we have

$$\begin{cases} 2c_f \left(\delta - \frac{v_y + l_f w}{v_x} \right) + 2c_r \left(\frac{l_r w - v_y}{v_x} \right) = m(\dot{v}_y + v_x w) \\ 2l_f c_f \left(\delta - \frac{v_y + l_f w}{v_x} \right) - 2l_r c_r \left(\frac{l_r w - v_y}{v_x} \right) = I_z \dot{w} \end{cases} \quad (38)$$

So, the 2-DOF model of tractor is

$$\dot{\mathbf{X}} = \mathbf{A}\mathbf{X} + \mathbf{B}\mathbf{u} \quad (39)$$

where, $\mathbf{X} = [\dot{v}_y \quad \dot{w}]^T$; $\mathbf{u} = \delta$;

$$\mathbf{A} = \begin{bmatrix} -\frac{2c_f + 2c_r}{mv_x} & -\frac{2c_f l_f - 2c_r l_r}{mv_x} - v_x \\ -\frac{2l_f c_f - 2l_r c_r}{I_z v_x} & -\frac{2l_f^2 c_f + 2l_r^2 c_r}{I_z v_x} \end{bmatrix}$$

$$\mathbf{B} = \begin{bmatrix} \frac{2c_f}{I_z} \\ \frac{2l_f c_f}{I_z} \end{bmatrix}$$

APPENDIX C

CALCULATION OF THE CUBIC SPLINE INTERPOLATION

We set the original expected curve of the tractor to be $f(x)$, and construct a curve $S(x)$ close to $f(x)$, which satisfies the same value as $f(x)$ at the interpolation point, and any two points are cubic curves. The second derivative of curve $S(x)$ with respect to x is continuous.

The function value of the $n + 1$ given points $a = x_0 < x_1 < \dots < x_n = b$ on $[a, b]$ is y_0, y_1, \dots, y_n . Then the function $S(x)$ through x_0, x_1, \dots, x_n satisfies the following equations:

(1) Interpolation continuity

$$S_i(x_i) = y_i \quad (i = 0, 1, \dots, n-1) \quad (40)$$

$$S_i(x_{i+1}) = y_{i+1} \quad (i = 0, 1, \dots, n-1) \quad (41)$$

(2) Differential continuity

$$S'_i(x_{i+1}) = S'_{i+1}(x_{i+1}) \quad (i = 0, 1, \dots, n-2) \quad (42)$$

$$S''_i(x_{i+1}) = S''_{i+1}(x_{i+1}) \quad (i = 0, 1, \dots, n-2) \quad (43)$$

The spline curve is

$$\begin{cases} S_i(x) = a_i + b_i(x - x_i) + c_i(x - x_i)^2 + d_i(x - x_i)^3 \\ S'_i(x) = b_i + 2c_i(x - x_i) + 3d_i(x - x_i)^2 \\ S''_i(x) = 2c_i + 6d_i(x - x_i) \end{cases} \quad (44)$$

where, $S_i(x)$ is the interval function of the subinterval $x_i \leq x \leq x_{i+1}$. The specific implementation steps are as follows.

Step 1: Measure the step length, and substitute the data point and endpoint conditions.

Substituting the step length $h_i = x_{i+1} - x_i$ into the condition of the spline curve, and according to Eq. (40), we have

$$a_i = y_i \quad (45)$$

According to Eq. (41), we have

$$a_i + b_i h_i + c_i h_i^2 + d_i h_i^3 = y_{i+1} \quad (46)$$

And according to Eq. (42), we have

$$\begin{cases} S'_i(x_{i+1}) = b_i + 2c_i h_i + 3d_i h_i^2 \\ S'_{i+1}(x_{i+1}) = b_{i+1} + 2c_{i+1} h_{i+1} + 3d_{i+1} h_{i+1}^2 = b_{i+1} \end{cases} \quad (47)$$

According to Eq. (47), we can further get

$$b_i + 2c_i h_i + 3d_i h_i^2 - b_{i+1} = 0 \quad (48)$$

Furthermore, according to Eq. (43), we have

$$2c_i + 6d_i h_i - 2c_{i+1} = 0 \quad (49)$$

Step 2: Calculate the coefficients of the spline curve.

Let $m_i = S''_i(x_i) = 2c_i$, and substitute it to Eq. (49) to get $m_i + 6d_i h_i - m_{i+1} = 0$. And we have

$$d_i = \frac{m_{i+1} - m_i}{6h_i} \quad (50)$$

Then, c_i and d_i are substituted into Eq. (46), and we obtain

$$b_i = \frac{(y_{i+1} - y_i)}{h_i} - \frac{h_i}{2} m_i - \frac{h_i}{6} (m_{i+1} - m_i) \quad (51)$$

b_i , c_i and d_i are substituted into Eq. (48), and we obtain

$$\begin{aligned} & h_i m_i + 2(h_i + h_{i+1})m_{i+1} + h_{i+1} m_{i+2} \\ & = 6 \left[\frac{(y_{i+2} - y_{i+1})}{h_{i+1}} - \frac{(y_{i+1} - y_i)}{h_i} \right] \end{aligned} \quad (52)$$

Therefore, a system of linear equations with m unknowns can be constructed. The coefficient of spline curve in Eq. (44) can be determined as

$$\begin{cases} a_i = y_i \\ b_i = \frac{(y_{i+1} - y_i)}{h_i} - \frac{h_i}{2} m_i - \frac{h_i}{6} (m_{i+1} - m_i) \\ c_i = \frac{m_i}{2} \\ d_i = \frac{m_{i+1} - m_i}{6h_i} \end{cases} \quad (53)$$

Step 3: Determine the boundary conditions to construct the equation.

From the value range of i , we have $n - 1$ formulas, but also have $n + 1$ unknown quantities m , which is needed to add constraints to get a unique path interpolation curve $S(x)$.

When the tractor signal is interrupted, the coordinates of the interruption point (the interpolation starting point coordinates) can be obtained, but it is difficult to obtain the coordinates of the signal recovery point (the interpolation end coordinates). So, the natural boundary conditions are selected as the end conditions, that is, the special case of the second boundary condition. The second derivative of the endpoint $a = x_0$ and $b = x_n$ of $f(x)$ is 0. The boundary of $S(x)$ should satisfy

$$\begin{cases} S(x_0) = f(x_0) \\ S(x_n) = f(x_n) \\ S''(x_0) = f''(x_0) = 0 \\ S''(x_n) = f''(x_n) = 0 \end{cases} \quad (54)$$

The equations to be solved can be expressed as

$$Am = 6E \quad (55)$$

where, A is the coefficient matrix;

$$m = [m_0, m_1, \dots, m_n]^T \quad (56)$$

$$E = \begin{bmatrix} 0 \\ y_2 - y_1)/h_1 - (y_1 - y_0)/h_0 \\ (y_3 - y_2)/h_2 - (y_2 - y_1)/h_1 \\ \vdots \\ (y_n - y_{n-1})/h_{n-1} - (y_{n-1} - y_{n-2})/h_{n-2} \\ 0 \end{bmatrix} \quad (57)$$

Therefore, the only interpolation curve $S(x)$ is obtained, that is, the path curve of the tractor in the case of signal interruption.

APPENDIX D

PROOF OF THEOREM 1

Proof: There is a symmetric positive definite matrix P , and let the control input be

$$u = K_i X \quad (58)$$

where

$$K_i = -\frac{1}{2}B_i^T P \quad (59)$$

According to $\bigcup_{i=1}^p \Omega_i = R^n \setminus \{0\}$, we have $\forall X \in R^n \setminus \{0\}$, there exists i_0 such that $X \in \Omega_{i_0}$; If $X(t) \in \Omega_i$, we have $\sigma(X(t)) = i$; If $X(t) \in \bigcap_{j=1}^k \Omega_{ij}$, then

$$\sigma(X(t)) = \arg \left\{ \min_{ij} Z_{ij}(X) < 0 \right\} \quad (60)$$

where the function $\arg(\cdot)$ represents the subscript value that satisfies the expression condition in the parentheses. Let the Lyapunov function be

$$V(X) = X^T P X \quad (61)$$

When $\sigma(X(t)) = i$, namely, the system switches to the i -th subsystem, we have

$$\begin{aligned} \dot{V}(X) &= 2X^T P \dot{X} \\ &= 2X^T P[(A_i + \Delta A_i)X + (B_i + \Delta B_i)u] \end{aligned} \quad (62)$$

Substituting Eq. (58) and Eq. (59) into Eq. (62), and it can be rewritten as

$$\dot{V}(X) = 2X^T P(A_i + \Delta A_i - \frac{1}{2}B_i B_i^T P + \Delta B_i K_i)X \quad (63)$$

Then, we substitute Eq. (19) into Eq. (63), and it can be rewritten as

$$\begin{aligned} \dot{V}(X) &= X^T [A_i^T P + P A_i - P B_i B_i^T P \\ &\quad + E_i^T F^T(t) D_i^T P + E_i^T F^T(t) D_i^T P \\ &\quad + P D_i F(t) E_i + K_i^T N_i^T F^T(t) M_i^T P \\ &\quad + P M_i F(t) N_i K_i] X \end{aligned} \quad (64)$$

According to Lemma 1 and Eq. (20), we have

$$\begin{aligned} &E_i^T F^T(t) D_i^T P + P D_i F(t) E_i \\ &\leq \varepsilon E_i^T F^T(t) F^T(t) E_i + \varepsilon^{-1} P D_i D_i^T P \\ &\leq \varepsilon E_i^T E_i + \varepsilon^{-1} P D_i D_i^T P \end{aligned} \quad (65)$$

and

$$\begin{aligned} &K_i^T N_i^T F^T(t) M_i^T P + P M_i F(t) N_i K_i \\ &\leq \gamma K_i^T N_i^T F^T(t) F(t) N_i K_i + \gamma^{-1} P M_i M_i^T P \\ &\leq 0.25\gamma P B_i N_i^T N_i B_i^T P + \gamma^{-1} P M_i M_i^T P \end{aligned} \quad (66)$$

Substituting Eq. (65) and Eq. (66) into Eq. (64), we can obtain

$$\begin{aligned} \dot{V}(X) &\leq X^T (A_i^T P + P A_i - P B_i B_i^T P + \varepsilon E_i^T E_i \\ &\quad + \varepsilon^{-1} P D_i D_i^T P + 0.25\gamma P B_i N_i^T N_i B_i^T P \\ &\quad + \gamma^{-1} P M_i M_i^T P) X < 0 \end{aligned} \quad (67)$$

Therefore, the closed-loop system is asymptotically stable and the proof is complete. ■

APPENDIX E FUZZY INFERENCE RULES

TABLE V: Fuzzy rule control table of K_p .

e \ ec	NB	NM	NS	ZO	PS	PM	PB
NB	PB	PB	PM	PM	PS	ZO	ZO
NM	PB	PB	PM	PS	PS	ZO	NS
NS	PM	PM	PM	PS	ZO	NS	NS
ZO	PM	PM	PS	ZO	NS	NM	NM
PS	PS	PS	ZO	NS	NS	NM	NM
PM	PS	ZO	NS	NM	NM	NM	NB
PB	ZO	ZO	NM	NM	NM	NB	NB

TABLE VI: Fuzzy rule control table of K_i .

e \ ec	NB	NM	NS	ZO	PS	PM	PB
NB	NB	NB	NM	NM	NS	ZO	ZO
NM	NB	NB	NM	NS	NS	ZO	ZO
NS	NB	NM	NS	NS	ZO	PS	PS
ZO	NM	NM	NS	ZO	PS	PM	PM
PS	NM	NS	ZO	PS	PS	PM	PB
PM	ZO	ZO	PS	PS	PM	PB	PB
PB	ZO	ZO	PS	PM	PM	PB	PB

TABLE VII: Fuzzy rule control table of K_d .

e \ ec	NB	NM	NS	ZO	PS	PM	PB
NB	PS	NS	NB	NB	NB	NM	PS
NM	PS	NS	NB	NM	NM	NS	ZO
NS	ZO	NS	NM	NM	NS	NS	ZO
ZO	ZO	NS	NS	NS	NS	NS	ZO
PS	ZO	ZO	ZO	ZO	ZO	ZO	ZO
PM	PB	NS	PS	PS	PS	PS	PB
PB	PB	PM	PM	PM	PS	PS	PB

APPENDIX F MAIN TRACTOR PARAMETERS

The main parameters of the tractor driving platform used in the experiment were listed as the following table.

APPENDIX G DETAILED FIGURES

The communication schematic diagram under TD mode was shown in Fig. 14. and the initial data record page near point A was shown in Fig. 15.

The main parameters of the unmanned tractor driving platform					
Tractor body	Model	CFD504A	IPC ^{1,2}	IPC 1	Processor RAM Hard disk COM Screen Model Processor RAM Hard disk COM
	Rated speed	2400 r/min			
	Wheelbase	2100 mm			
	Engine rated power	36.8 KW			
Main measurement unit	Wheel base (front wheel)	1410 mm	Drive unit	IPC 2	Intel i7 8G 256G SSD RS422/485 12.1 inch NK350-1 Intel i7 4G 256G SSD RS422/485
	Wheel base (rear wheel)	1400 mm			
	Calibrated traction	12.5 kN			
	Driving speed (forward)	2.18 31.16 km/h			
	Driving speed (backward)	1.92 km/h			
	Overall dimensions (length×width×height)	3602×1700×2268 mm			
	Attitude accuracy	0.1° (Baseline length ≥ 2)			
	Positioning accuracy	Single Point L1/L2: 1.2 m DGPS: 0.4 m RTK: 1 cm +1 ppm			
	Data update rate	100 Hz			
	Initialization time	Less than 1 min			
Main measurement unit	GNSS	Integrated navigation accuracy	Visual unit ³	Model	Intel D435 10 m 1920 × 1080 87° × 58°
	Lidar	Modle			
		Sampling rate			
		Laser wavelength			
		Measurement accuracy			
		Measurement resolution			
Angle sensor	Angle sensor	Output signal			
		Power supply			
		Minimum resolution			
Signal delay	Signal delay	Signal delay			
		0.5 - 4.5 VDC			
		4.5 - 5.5 VDC			
Signal delay	Signal delay	0.1°			
		0.3 ms			
		0.3 ms			

1. In the tractor dual-mode driving platform, the IPC 1 (Industrial Personal Computer) is placed at the SD end of the tractor, which is mainly used to receive remote control commands, signal transmission and SD control. The IPC 2 is placed at the TD control end, which is responsible for collecting and sending remote control instructions, monitoring the working state of the tractor, etc.
2. The cloud platform used in the TD subsystem is the Alibaba Cloud Service, which specific configuration are: 1 core (vCPU), 2G (RAM), 1-5M (Bandwidth), 40G (System memory).
3. A depth camera of Intel D435 is used in the vision unit, which can collect the real-time working state of the tractor for the TD mode, and also can provide visual navigation information for the SD mode.

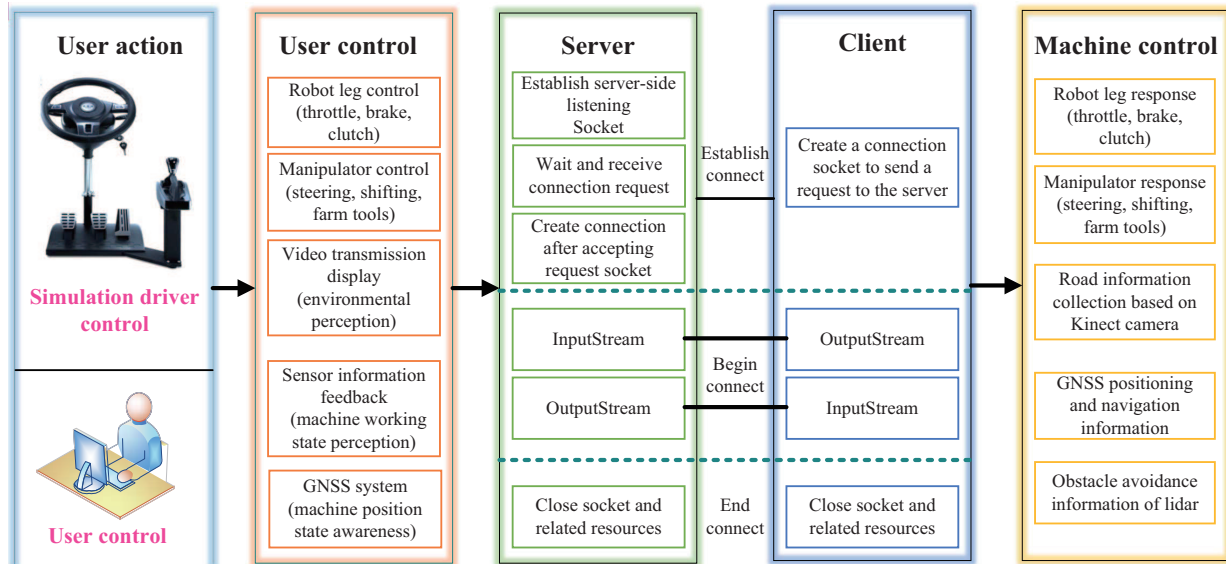


Fig. 14: Communication schematic diagram under TD mode.

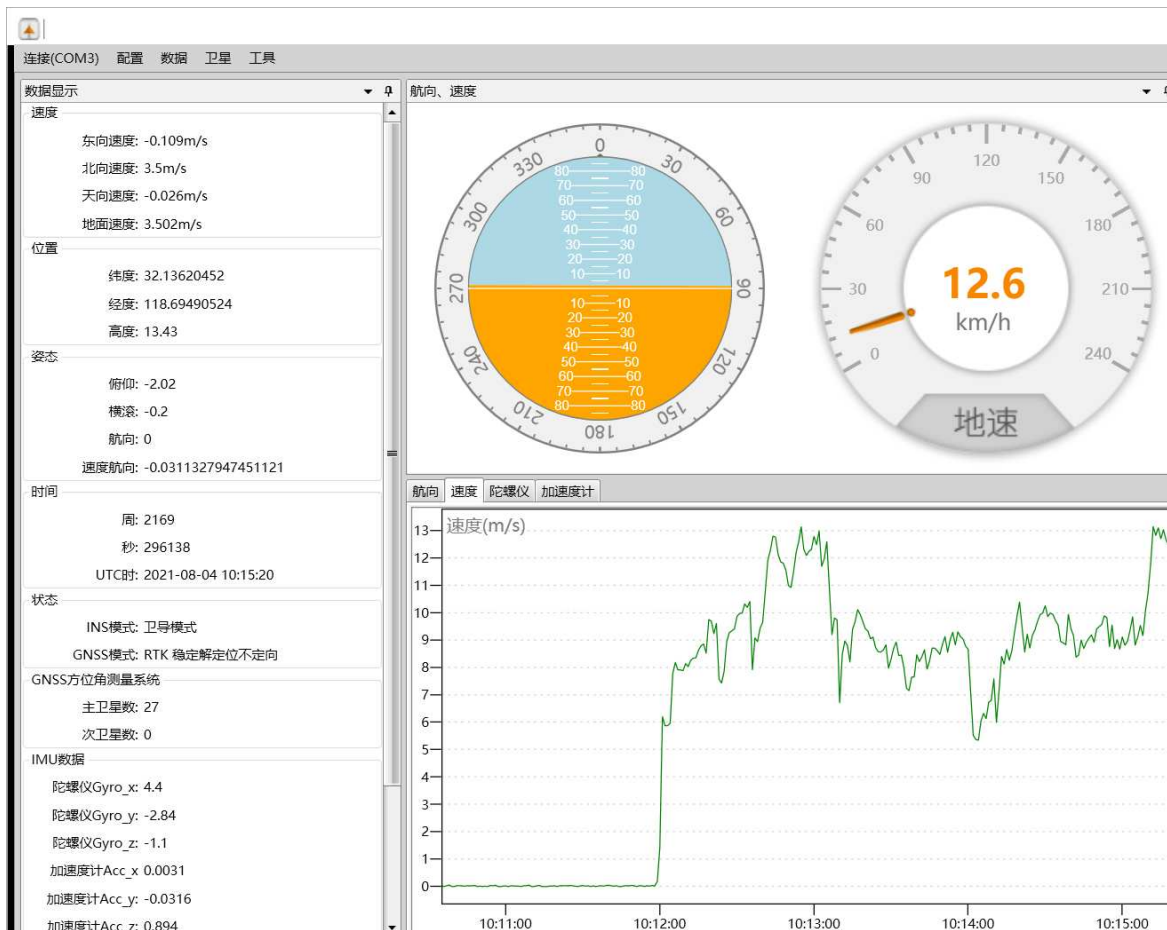


Fig. 15: The initial data record page near point A.